Proceedings of the Ninth IASTED European Conference
Power and Energy Systems (EuroPES 2009)
September 7 - 9, 2009 Palma de Mallorca, Spain

A MATHEMATICAL MODEL FOR CONDITION MONITORING OF A POWER TRANSMISSION LINE

Petronio Vieira Junior*, Miguel Angel Sanz Bobi **, Roberto Célio Limão* and Martin Max Luiz de Castro Negrão*
* Federal University of Pará
Augusto Corrêa, 1, ZIP 66.075-900
Belém / Pará – Brazil
**Pontificia Comillas University
Santa Cruz de Marcenado, 26, ZIP 28.015
Madrid / Spain
petronio@ufpa.br, masanz@dsi.icai.upcomillas.es, limão@ufpa.br, max@ufpa.br

ABSTRACT
This paper describes the development of a mathematical model for the on-line condition monitoring of electric power transmission lines (TL). It includes environmental considerations in the normal conditions of the TL operation. This mathematical model is intended to be used in the verification in real time of the operation conditions of TL among two electrics substations (SEs). Different meters are installed in the SEs synchronized by GPS from where data is acquired concerning the variables that should be monitored and it also allows the validation and training of the model. Therefore this model should assist a method that will allow for maintenance predictions, based on reliability at a low cost. It will also allow verification the result of the interventions of maintenance, checking the efficiency of this in activities such as cleaning insulators. The goal of this paper is to describe the model obtained, its validations and fitting.

KEY WORDS
Mathematical model, condition monitoring, power transmission.

1. Introduction

Maintenance applied to transmission lines (TL) is based usually on inspections according to a preventive maintenance scheduling and on corrective maintenance actions. This paper describes a mathematical model for condition monitoring of a power TL that could be used as part of a predictive maintenance plan. This model is based on the continuous monitoring of a power TL using equipment installed in the electrical substations (SEs) at the ends of the TL. This new methodology proposed is named On-line Condition Monitoring of Transmission Lines (MOLLT - *Monitoração On-Line de Linha de Transmissão*), and it allows for low cost predictive maintenance planning based on sensors already used for other monitoring purposes of the TL. This methodology consists of verifying in real time the condition of a TL through the indirect measurement of its leakage current. As the measurement is on-line, the verification of the conditions of the TL in real time makes it possible to share this information between operation and maintenance, following the current technological tendency used in automated systems, optimizing the maintenance planning and reducing its costs. This paper describes the concepts and development of the mathematical model used for condition monitoring of a power TL that allows the prediction of faults.

2. Model for fault prediction of a TL

The most advanced methodology for fault prediction of an industrial system monitored on-line corresponds to the diagram of blocks described in figure 1. This methodology consists of comparing the results of the mathematical model that simulates the real behaviour of the system with its real performance. It is verified if the difference observed in real-time corresponds either to a normal or an abnormal behaviour, and then the situation is diagnosed. This diagnostic will be very important for a possible prediction or prognosis of evolution of the current condition of the system.

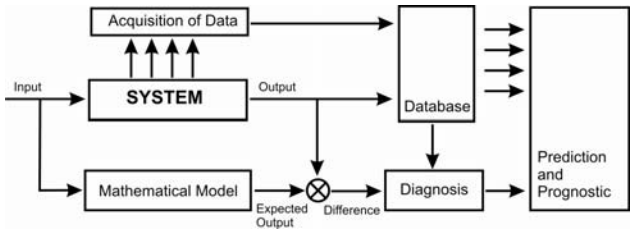

Fig. 1 – Diagram of blocks for fault detection.

A TL can be considered as a system whose function is the transport of electric energy. Its continuous monitoring through representative parameters is very important to assess its condition. The research presented in this paper proposes the observation of representative parameters able to indicate if the TL is in good condition for operation or not. These parameters are used in the mathematical model of the TL developed for the prediction of its condition. Traditionally a TL model is developed keeping constant the resistance, inductance and capacitance values. The reason for this is that these values characterize the electric circuit for which is established an electrical current and a voltage supplying a load.

Therefore the variables that are used in the conventional models are voltage and current. A model for the prediction of the TL condition should have as variables the resistance and the capacitance, because these are parameters that can evaluate the integrity of the circuit. The function of the resistance is to offer continuity to the passage of the current for the line and the function of the capacitance is to provide electric insulation for the passage of the current. Therefore, resistance monitoring can be used for the detection of problems in connections and the corona effect, while the capacitance monitoring could detect defects for example in the isolation level due to leakages or pollution in the insulators, or due to burning. Therefore the model developed should contemplate the behaviour of the resistance and the capacitance of the TL. Here then a practical question appears: how can the resistance and the capacitance of a line in operation be measured? Of course this should be done through an indirect measurement. Then which will be the variable to be observed for anomaly detection and diagnosis? These questions are addressed and answered in the next sections of this paper.

3. Diagnostic parameters

The main variable to be observed to verify the condition of a power TL used in MOLLT is the leakage current. Through its monitoring it is possible to evaluate the isolation conditions of the TL. Applying the law of Gauss, the leakage current corresponds to the difference among the input and output currents in a LT, as is shown in figure 2.

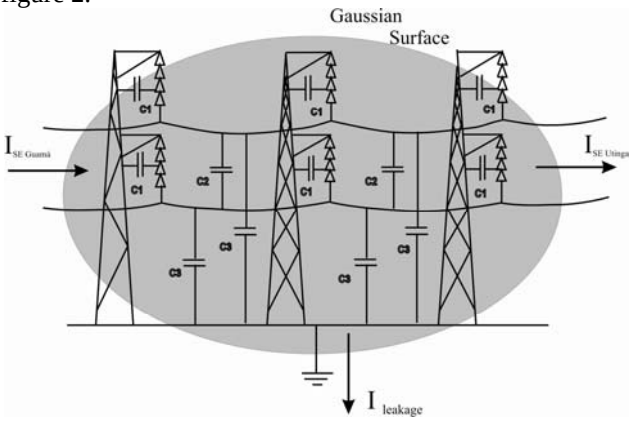

Fig. 2 – Simplified scheme to obtain the leakage current in a TL.

The typical wave shape of the leakage current measured in a TL of a length of approximately 20 Km and 230kV is shown in figure 3. Previous studies [1] have demonstrated that by using a harmonic decomposition of the leakage current, it is possible to detect and to locate a defect. However the measurements already made include some variations in the harmonic measurements that do not represent a defect in a TL. In figures 4 and 5 the harmonic decomposition of the leakage current of a TL can be observed in two different moments of a TL operation on the same day (230kV, 200A).

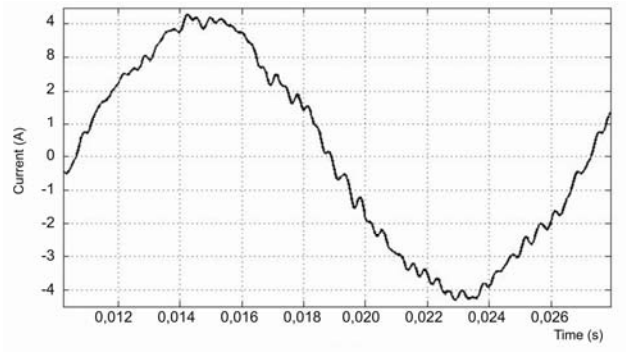

Fig. 3 – Wave shape of the leakage current.

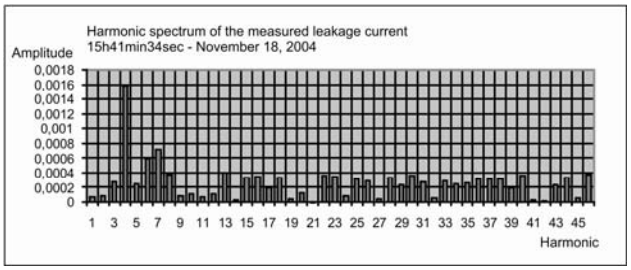

Fig. 4 – Harmonic decomposition during the afternoon.

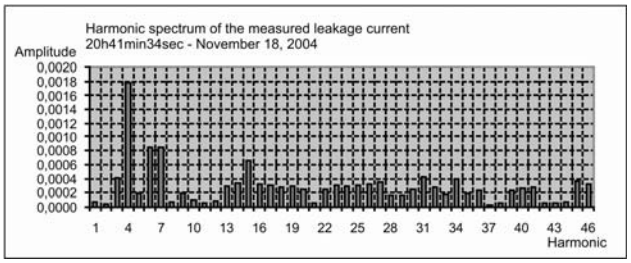

Fig. 5 – Harmonic decomposition during the night time.

In spite of the amplitude of the leakage current it was practically the same during the afternoon and the night time periods, 4,0442A and 4,0591A, respectively. However, the harmonic decompositions present some very different amplitude, particularly in the frequencies above 1.800 Hertz, where defects typically are discovered in the insulators of a TL [2]. Analyzing the conditions in which the measurements were accomplished, the change was observed only in the environmental conditions. These real measurements reinforce the need to consider the environmental variables in the model of fault prediction of a TL.

4. Tests for capacitance observation

In order to know the influence of environmental conditions on the capacitance of a TL, an experimental facility was built. This consists basically of a capacitor installed in an environment where it is possible to control the temperature (T), the air relative humidity (UR) and the wind speed (W). A schematic design of this facility is presented in figure 6.

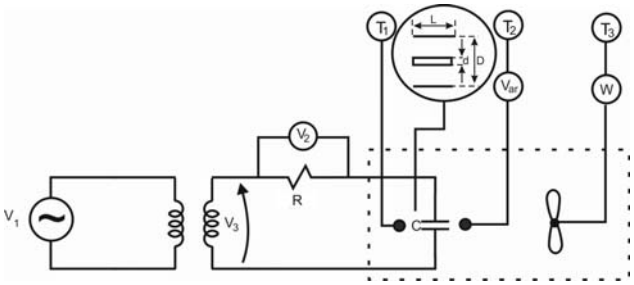

Fig. 6 – Schematic design for capacitance verification.

A voltage controlled source of value V1 and a frequency of 60 Hz can supply a voltage V3 through a Potential Transformer (TP). The voltage V3 is applied to the terminals of a resistor of known value (R) and to a capacitor of unknown value (C) both connected in series. The voltage V2 is measured and determined the current circulating. All of this allows for the calculations of the value of C using the physical dimensions and the relative permittivity of the air. The measurements are made for several voltage levels and conditions of UR, T and W. The capacitor is coax type with an acrylic cone to drive the air, as described in figure 7. The capacitor length is 10 times larger than its diameter in order to consider the spread effect to be negligible [3]. The coax capacitor is installed in an acrylic box, called the test box, where the environmental conditions are controlled.

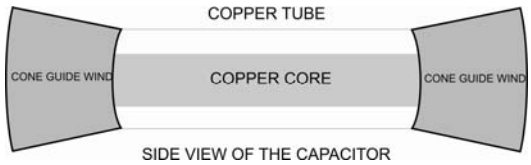

Fig. 7 – Test Capacitor.

The facility includes an electronic device to control and to measure several variables, as is shown in the diagram of blocks of figure 8. Figure 9 shows a photo of the facility used including an anemometer and a term-hydrometer on the test box.

5. Capacitance behaviour

By using the test box it was possible to carry out measurements to verify the behaviour of the capacitance changing the environmental conditions. Through TP it was possible to obtain data for a range of voltage from 100 to 10.000V. One of the important conclusions that could be obtained is that in the voltage range below 5kV the behaviour of the conditions of the air permittivity is different than in the range above this value. This can be observed in figures 10 and 11 that show the behaviour of the capacitance with the wind speed and relative humidity respectively. This conclusion indicates that there exists the possibility that this phenomenon can be repeated for a voltage value of 230kV, and that it is the amplitude of the voltage of operation of the TL that will validate the model.

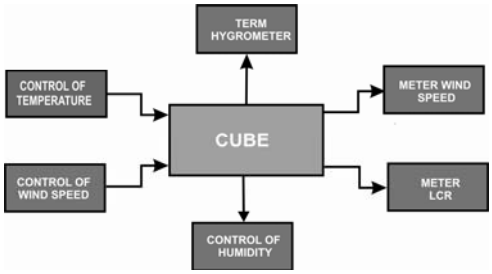

Fig. 8 – Test box instrumentation.

Fig. 9 - Experimental facility for verification of the capacitance.

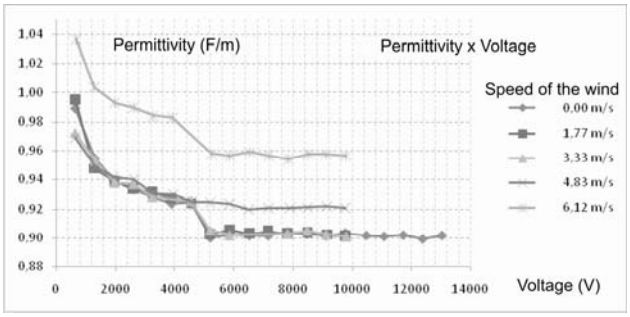

Fig. 10 – Behaviour of capacitance with the wind speed.

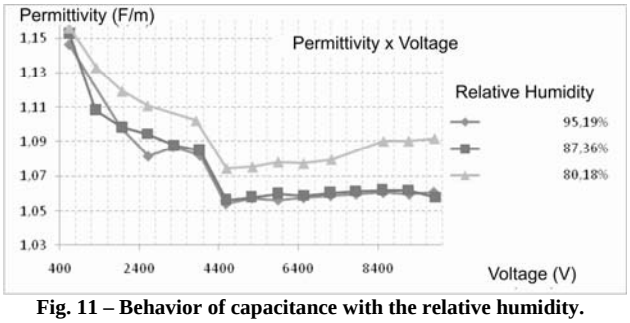

Fig. 11 – Behavior of capacitance with the relative humidity.

For this reason the conclusions regarding these measurements should be limited to the knowledge of the tendencies of the capacitance behavior. In this sense with the aid of the graphs obtained, it can be affirmed, for example, that the permittivity rises with the increase of the speed or the relative humidity of the air and that the effects are cumulative, in other words, when for a certain speed the humidity increases, the permittivity increases

[3] and [4]. For this reason the measurements were taken and analyzed separately.

Starting from this initial analysis empiric, equations were obtained from the observation of the behavior curves presented in figures 12, 13 and 14 that correspond to the permittivity behaviour in relation to the variation of the temperature, relative humidity of the air and wind speed, with the voltage. Initially a rotation was accomplished in each one of the previous curves for a better observation of the variation. This is presented in figures 15(a), 16(a) and 17(a). Afterwards it is put upon a curve to characterize the behavior of the variable, as shown in figure 15(b), for temperature, 16(b) for relative humidity of the air and 17(b) for the wind speed. The obtained equations are:

$$k_d(T) = 5 \times 10^{-5}T^2 + 62 \times 10^4 T + 0.51354 \quad (1)$$

$$k_d(U_{ar}) = 5 \times 10^{-5}{U_{ar}}^2 - 9{,}5 \times 10^{-3}U_{ar} + 1.06144 \quad (2)$$

$$k_d(W) = 2 \times 10^{-4}W^2 + 12 \times 10^{-4}W - 0{,}2979 \quad (3)$$

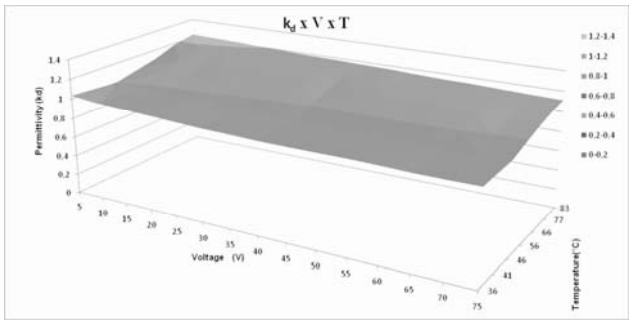

Fig. 12 – Behavior of the capacitance with the temperature and voltage.

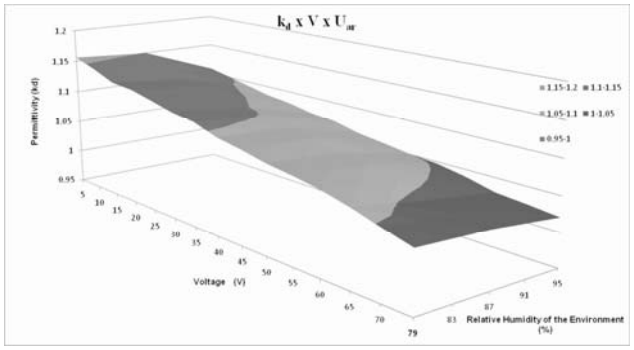

Fig. 13 – Behavior of the capacitance with the relative humidity of the air and the voltage.

The factors K_d(T), K_d(U_{ar}) and K_d(W) are applied on the value of the permittivity of the air of the TL capacitance.

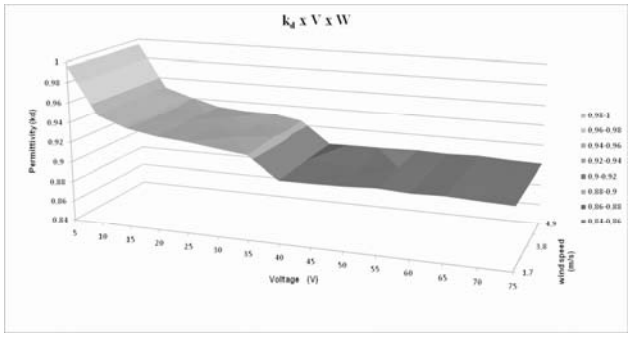

Fig. 14 – Behavior of the capacitance with wind speed and voltage.

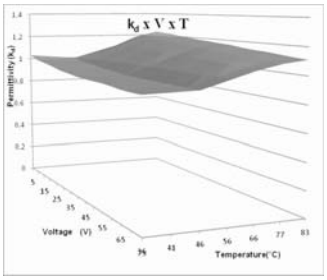

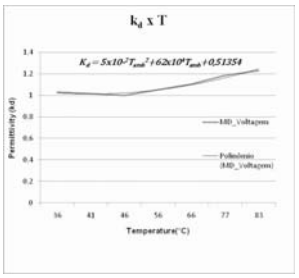

(a) Rotating figure 11 **(b) Placed on a lineal curve**

Fig. 15 – Analysis of temperature variation.

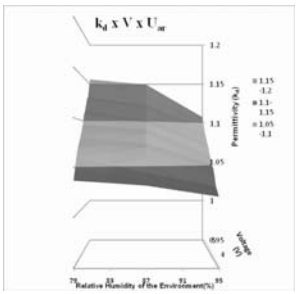

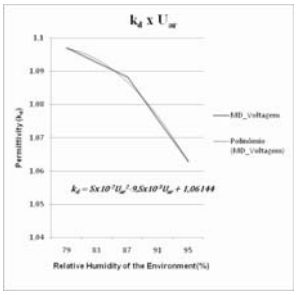

(a) Rotating the figure 12 **(b) Placed on a lineal curve**

Fig. 16 – Analysis of the variation of the relative humidity with the voltage.

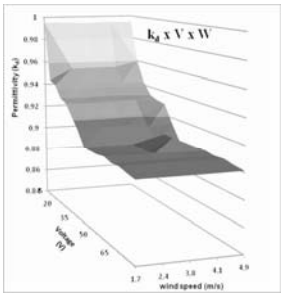

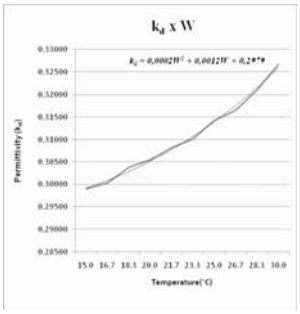

(a) Rotating the figure 13 **(b) Putting upon a lineal curve**

Fig. 17 – Analysis of the variation of the speed of the wind with the voltage.

6. Behavior of the Resistance

A cable reaches a temperature in permanent regime when there is a balance among gained and lost heat for the cable. A cable generates heat, mainly, due to the Joule effect $q_j = I^2R\ [W/km]$ and due to the solar radiation $q_s\ [w/m]$ and it loses heat for two known mechanisms [3]: irradiation $q_r\ [W/m]$ and convection $q_c\ [W/m]$. The equation balance will be:

$$I^2R + q_s = q_r + q_c \quad (4)$$

of which is obtained: $R = \sqrt{\frac{q_r + q_c - q_s}{I}}$ (5)

7. Mathematical Model

The mathematical model is developed in the time domain using an equivalent circuit in PI configuration. It considers the insulator as being a capacitor in parallel with a resistor, as is shown in figure 18. In this scheme the line losses can be represented by the leakage current (I_C) and the conduction (I_R).

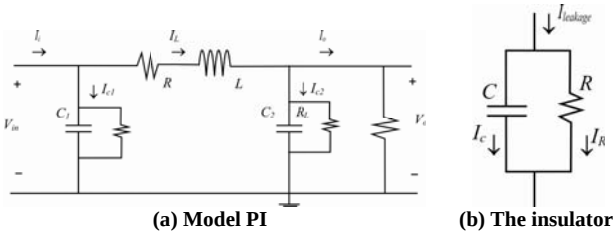

(a) Model PI **(b) The insulator Model**

Fig. 18 – Models used in the numeric simulation.

This model was validated using real data obtained from a power TL located in the Brazilian Amazonian between the SEs of Guamá and Utinga of the Tucuruí transmission system of 230 kV (TUC 86 - 3003R - 5), described in figure 19. It belongs to the system of transmission of the Electric Central of the North of Brazil - ELETRONORTE.

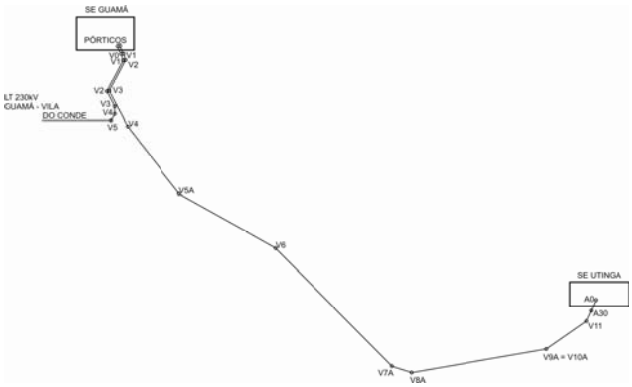

Fig. 19 –Transmission Line used for the experiment.

The Utinga-Guamá line possesses 50 towers with a medium distance among the towers of 213.64 m, with a total length of 19,04316 km. The values of the elements of the circuit R, L and C used in the numeric simulation were obtained using the distances and relative position among the cables and between the cables and the ground and the cable earth. The calculations of R, L and C were done considering a single structure, the tower type SOD (39 towers), presented in figure 20.

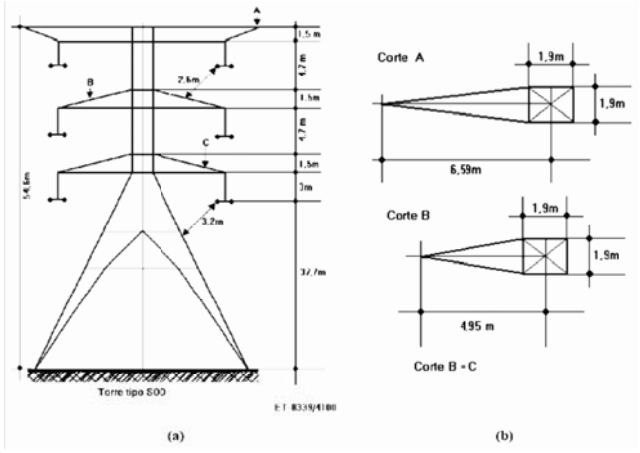

Fig. 20 – Design of the tower for determination of the distances among the cables, these to the ground and the cable earth.

The values obtained theoretically through calculations of the matrix equations described in [4] are:

Capacitance: 6,13 x 10^{-9} F/km

Resistance: 1,07808 Ω

Inductance: 0,026143 H/km

The matrix equations used above for the calculation of the elements R, L and C possess a series of simplifications. In the case of the capacitance, the matrix equation used does not consider the effect of the resistivity and the effect of ray for the cable. A numeric method that considers these two effects is based on finite elements (FEM), whose development [6] and [7] are presented in figure 21.

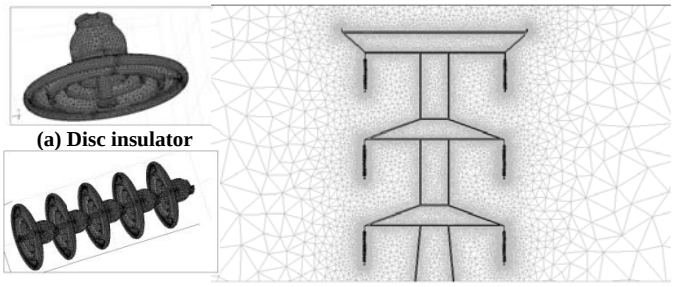

(a) Disc insulator **(b) String of disc insulator** **(c) Tower type SOD in FEM**

Fig. 21 – Using finite elements for determination of the capacitance of the line.

For the method of the finite elements, the service capacitance for each circuit was calculated as 3,1992x10-09 (F/km). The calculation for an insulator using the method of the finite elements was validated by the experimental measurements obtained applying voltage in industrial frequency. This is shown in figure 22.

Fig. 22 – Insulator in test for verification of the capacitance.

8. Model Simulation

The model was simulated using the MATLAB – Simulink software. The dynamic equations, extracted from the equivalent circuit of figure 18, use the output voltage and current of the SE Guamá as voltage V_i and I_i, respectively. The input voltage and the current to the SE Utinga are represented as V_o and I_o, respectively. Figure 23 shows the diagram of blocks using Simulink [8]. The diagram of blocks shown in figure 23 has the values of R, L and C of the TL. However, if it is necessary to use this model for fault localization, the values of R, L and C should become separated many times to be analyzed in the TL. This

effect is represented in the Simulink diagram of blocks shown in figure 24, where each block, called a tower, is a subsystem with the same structure as the one shown in figure 23.

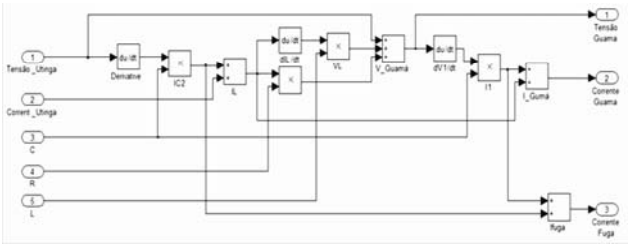

Fig. 23 – Basic Block of Simulink of the mathematical model.

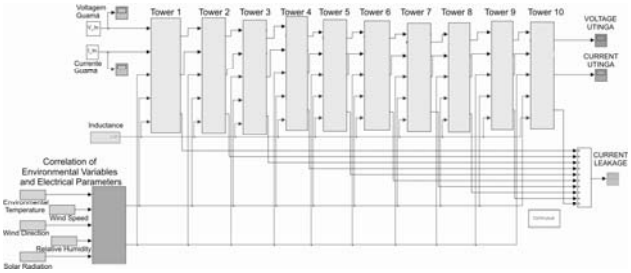

Fig. 24 – Blocks of Simulink for simulation for fault localization.

Figure 25 presents the form of wave of the TL three-phase current leakage obtained by simulation.

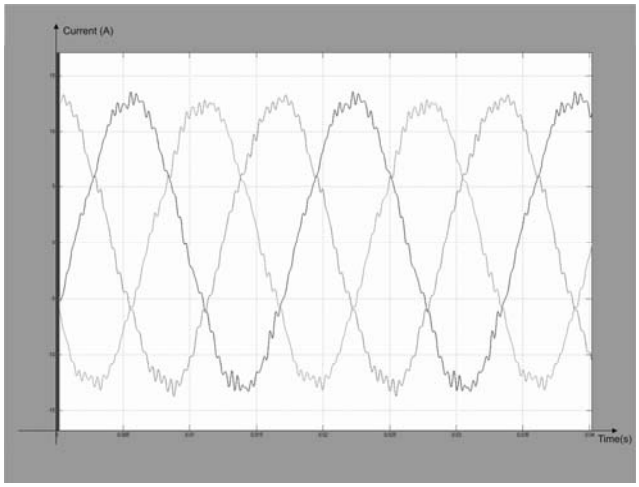

Fig. 25 – Form of wave of the three-phase leakage current obtained by simulation.

In the equations used, it is necessary to take into account the environmental variables, as described in equations 6, 7 and 8.

$$I_{C2} = C_2(T_{amb}, U_{rm})\frac{dV_2}{dt} \quad (6)$$

$$I_{C1} = C_1(T_{amb}, U_{rm})\frac{dV_1}{dt} \quad (7)$$

$$V_L = R(T_{amb}, U_{rm}).I_L + L.\frac{dI_L}{dt} \quad (8)$$

Equations 6 and 7 are introduced in the simulation as described in the diagram of blocks of figure 26.

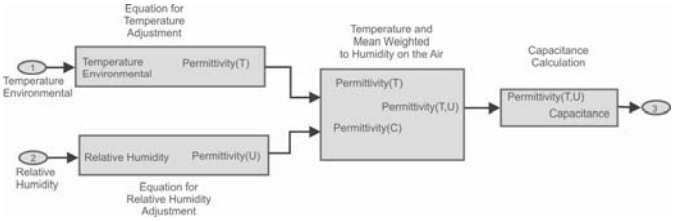

Fig. 26 – Environmental data inserted in the calculation of the resistance and capacitance.

The calculation of the variation of the resistance with the environmental variables is accomplished applying the measurements of the environmental conditions mentioned in equations 4 and 5, from where table 1 can be built with the aid of MATLAB through Simulink described in figure 27.

Table 1 – Behavior of the electric Resistance, according to suggested environmental variations (Ohm).

Speed of the wind (m/s)	Environment Temperature (°C)						Direction of the wind
	20	23	25	28	31	33	
3	1,837	1,901	1,918	1,950	1,971	1,990	90°
8	1,829	1,843	1,860	1,880	1,889	1,904	60°
10	1,815	1,827	1,838	1,853	1,880	1,895	45°
12	1,809	1,819	1,835	1,845	1,853	1,861	30
Speed of the wind (m/s)	250	300	350	400	450	500	Direction of the wind
	Radiação Solar (W/m^2)						

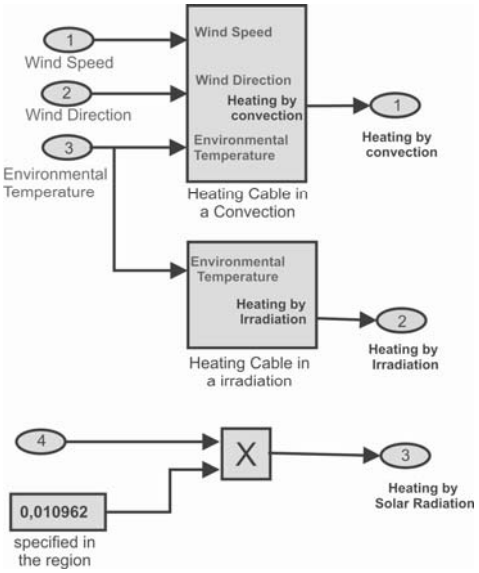

Fig. 27 - Responsible blocks for the calculation of the amount of heat loosened by each process of transmission suffered by the cable.

9. Experimental Implementation

The model validation is verified by the comparison between the results of numeric simulations and the experimental measurements. The experimental measurements were carried out through energy quality meters installed in the SEs of the Guamá and Utinga, synchronized by GPS, whose data are transmitted through the intranet of ELETRONORTE, using the arrangement described in figure 28.

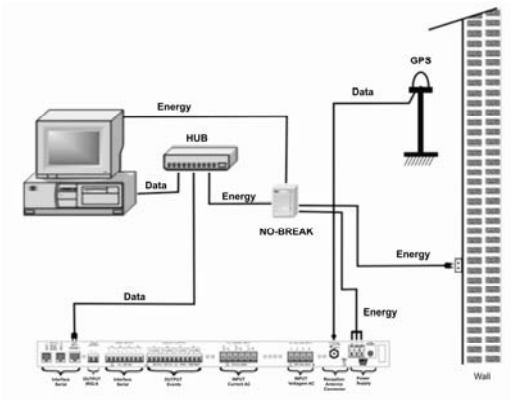

Fig. 28 – Connection arrangement for transmission of the data of the meters.

The installation of the energy meters in the SE Guamá is shown in figure 29.

(a) GPS antenna

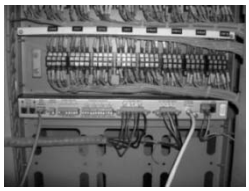

(b) Meter inside the electrical closet..

Fig. 29 – Installation of the meter of energy in SE Guamá.

The measurements of the environmental variables were accomplished with Remote Meteorological Stations - EMRs, as shown in figure 30. They include a multi-sensor for humidity acquisition, temperature, speed and direction of the wind, and a sensor of solar radiation. This information is stored in a dataloger and transmitted by radio with a reach of 16 km. EMRs are fed through solar panels.

Fig. 30 – Remote Meteorological Station (EMR) in operation test.

The data transmission of the Arbiter meter is accomplished through the intranet of the ELETRONORTE. The data of EMRs are transmitted by radio, until the SE where they are incorporated to the network, as is shown in figure 31.

10. Adaptation of the Capacitance Value to 230kV

Environmental data were obtained from EMRs and compared with those obtained from the test box. Figure 32 shows the comparison among these data in relation to the permittivity varying with the temperature. A similar behaviour is observed for the two curves taking into account that the curve described by the data obtained from the EMRs is at a different level. This confirms the considerations presented in section 4, through figures 10 and 11, and it indicates the existence of change levels of the permittivity according to levels of different voltages. Therefore the values of the permittivity of the air (TL capacitance) were adjusted for the values obtained from the EMRs.

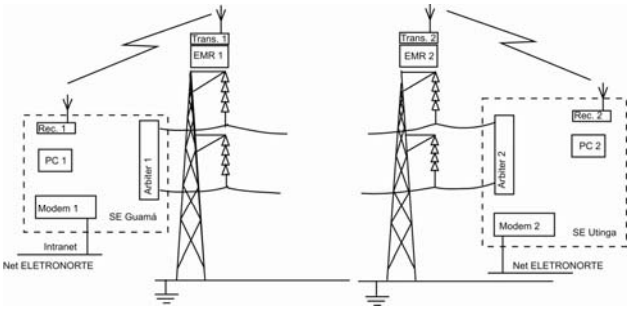

Fig. 31 - Transmission of the monitoring data.

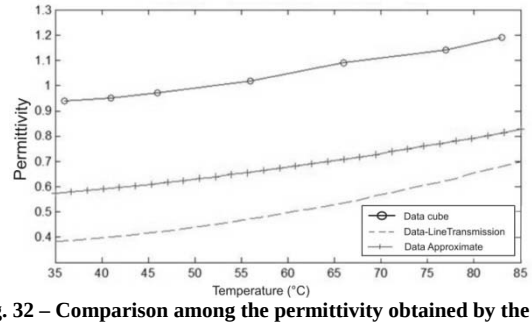

Fig. 32 – Comparison among the permittivity obtained by the test box and obtained by EMRs in relationship with the variation of the temperature.

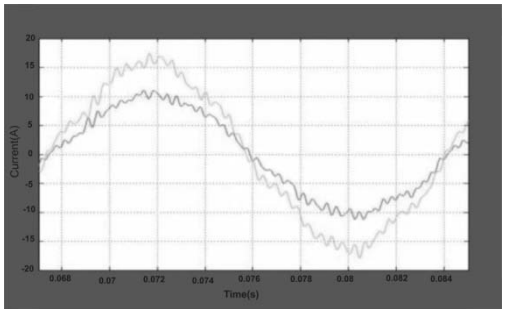

Fig. 33 – Overlap in the waves of the measured current and calculated current, considering the test box values.

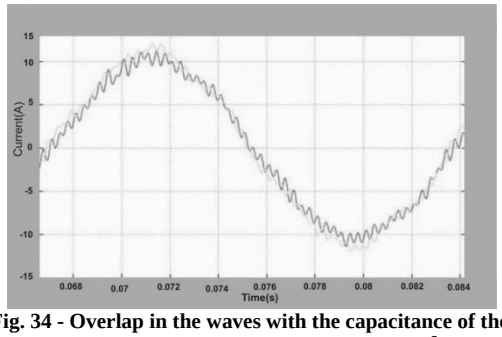

Fig. 34 - Overlap in the waves with the capacitance of the mathematical model adjusted to $20 \times 10^{-9} F$.

This adjustment was accomplished observing the leakage current. In figure 33 a comparison is observed among the leakage current obtained by measurement and those obtained experimentally using the values of the permittivity of the test box. In figure 34 the form of the wave of the leakage current is obtained theoretically using the values of the permittivity corrected by figure 32.

11. Experimental Validation

The objective of this model is the verification of the conditions of operation of TL through the observation of leakage current, as shown in figure 3. So it is necessary to decompose the leakage current in harmonic components and to analyze the variations of the several amplitudes in order to obtain recognition patterns. The model without considering the environmental variables did not allow to recognize the patterns in normal conditions as can be observed in item 2 through figures 4 and 5 at the highest frequencies. Figure 35 describes the harmonic decomposition of the leakage current obtained theoretically using the environmental variables.

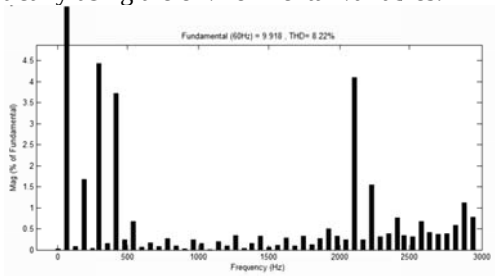

Fig. 35 - Harmonic decomposition of calculated leakage current.

These data were obtained on November 11, 2008, at 9h 20min with temperature 33°C, relative humidity 65%, wind speed (to or up 10m) $10\ m/s$, direction of the wind $80\ oNV$, solar radiation of $380\ W/m^2$. Figure 36 describes the harmonic decomposition of the leakage current obtained by measurement. Improvements were observed in the main amplitudes and more particularly in one of the higher frequencies, where more defects in the insulators are noticed.

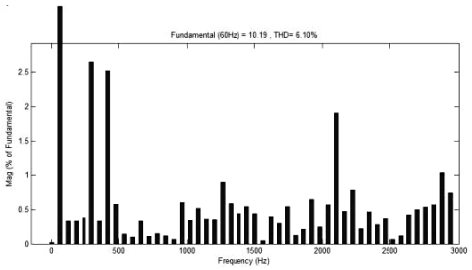

Fig. 36 - Harmonic decomposition of measured leakage current.

12. Conclusion

The verification method of the TL condition through the harmonic decomposition of the leakage current has been demonstrated to be successful. However in order to be used for a on-line monitoring of a TL, it is necessary to include some improvements in the model. For this reason, the characterization of the capacitance for the variation of the environmental conditions was incorporated. The adjustment required verified the value of the permittivity of 230kV, in spite of the behavior of the permittivity, to be the same ones for the range of voltage variation. The result of the introduction of the environmental variables in the model was a better representation of the harmonic in the highest frequencies in which the defects in the insulators are noticed. It is necessary to obtain more values and characterization of defects for the consolidation and use of the method proposed. Considering that TL are dynamic systems in this model, it is still necessary to increase the training for adjustment throughout the useful life of the TL.

Acknowledgements

The authors would like express their gratitude to the financial and technical support provided by ELETRONORTE for the development of the MOLLTs and IFPTL research projects and the institutional support of the Brazilian Government through the Coordination of Improvement of Personnel of Superior Level - CAPES.

References

[1] Cristiane Ruiz Gomes, *Localização de Falhas em Linhas de Transmissão Utilizando Decomposição Harmônica e Redes Neurais Artificiais*, Dissertação de Mestrado, Faculdade de Engenharia Elétrica, UFPA, Belém, 2006.

[2] Asenjo E. S., N. Morales O., Low Frequency Complex Fields In Polluted Insulators, *IEEE Transactions on Electrical Insulation, vol. EI-17*, No. 3, june 1982. Pág. 262 a 268.

[3] Martin Max Luís de Castro Negrão, *Modelo Matemático de Linhas de Transmissão Contemplando Influências Ambientais*, Dissertação de Mestrado, Faculdade de Engenharia Elétrica, UFPA, Belém, 2009.

[4] Murray W. Davis, A New Thermal Rating Approach: The Real Time Thermal Rating System for Strategic Overhead Conductor Transmission Lines, *IEEE Transactions on Power Apparatus and Systems, Vol. PAS-97*, no. 2, March/April 1978

[5] Fuchs, R. D., *Transmissão de Energia Elétrica: Linhas Aéreas;Teoria das Linhas em Regime Permanente*, 2ª edição. Rio de Janeiro, Livros técnicos e científicos, 1979.

[6] CORREA S. M. *Análise de Elementos Finitos para Determinação da Capacitância de Linhas de Transmissão. 2003. Dissertação de Mestrado*, Faculdade de Engenharia Elétrica, UFPA, Belém, 2004.

[7] Vieira Jr. P., Gomes, C. R., Côrrea, S. M., Gomes Jr., L. A., Computation of Capacitance of a Transmission Line using the Finite Element Method, *In: International Conference on Condition Monitoring and Diagnosis – CMD*, Changwon, 2006.

[8] Lucélio Albuquerque Gomes Junior, *Modelo Matemático de Linhas de Transmissão para Monitoração em Tempo Real, Dissertação de Mestrado*, Faculdade de Engenharia Elétrica, UFPA, Belém, 2007.